(9) Mohajer, Y.; Tyagi, D.; Wilkes, G. L.; Storey, R. F.; Kennedy, J. P. *Polym. Bull.* **1982**, *8*, 47.
(10) Bagrodia, S.; Pisipati, R.; Wilkes, G. L.; Storey, R. F.; Kennedy, J. P. *J. Appl. Polym. Sci.* **1984**, *29*, 3065 and references therein.
(11) Shilov, V. V.; Dmitruk, N. V.; Tsukruk, V. V.; Polyatskova, N. V.; Lipatov, Y. S. *Polym. Commun.* **1985**, *26*, 28.
(12) Jérôme, R.; Horrion, J.; Teyssié, P. In *Structure and Properties of Ionomers*; Pineri, M., Eisenberg, A., Eds.; NATO ASI Series C198; D. Reidel: Dordrecht, 1987; p 321 and references therein.
(13) Williams, C. E.; Russel, T. P.; Jérôme, R.; Horrion, J. *Macromolecules* **1986**, *19*, 2877.
(14) Ledent, J.; Fontaine, F.; Reynaers, H.; Jérôme, R. *Polym. Bull.* **1985**, *14*, 461.
(15) Williams, C. E. In *Contemporary Topics in Polymer Science*; Vol. 6; Culbertson, W. M., Ed., Plenum: New York, in press.
(16) Broze, G.; Jérôme, R.; Teyssié, P.; Gallot, B. *J. Polym. Sci., Polym. Lett. Ed.* **1981**, *19*, 415.
(17) Moudden, A.; Levelut, A. M.; Pineri, M. *J. Polym. Sci., Polym. Phys. Ed.*, **1977**, *15*, 1707.
(18) Selb, J.; Gallot, Y. In *Developments in Block Copolymers-2*, Goodman, I., Ed.; Elsevier Applied Science: London, 1985, Chapter 2.
(19) Lipatov, Y. S.; Shilov, V. V.; Oleinik, S. P.; Bogdanovich, V. A.; Shelkovnikova, L. A. *Vysokomol. Soedin., Ser. A* **1986**, *28*, 2242.
(20) Yu, X.; Nagarajan, M. R.; Li, C.; Gibson, P. E.; Cooper, S. L. *J. Polym. Sci., Polym. Phys. Ed.* **1986**, *24*, 2681.
(21) Venkateshwaran, L. N.; Feng, D.; Wilkes, G. L.; Leir, C. E.; Stark, J. E. *Polym. Prepr. (Am. Chem. Soc., Div. Polym. Chem.)* **1987**, *28*(2), 240.
(22) Fielding-Russel, G. S.; Pillai, P. S. *Polymer* **1977**, *18*, 859.
(23) Isono, Y.; Tanisugi, H.; Endo, K.; Fujimoto, T.; Hasegawa, H.; Hashimoto, T.; Kawai, H. *Macromolecules* **1983**, *16*, 5.
(24) Allen, R. D.; Yilgor, I.; McGrath, J. E. In *Coulombic Interactions in Macromolecular Systems*; Eisenberg, A., Bailey, F. E., Eds.; American Chemical Society: Washington, D.C. 1986; ACS Symp. Ser., 302, p 79.
(25) Khan, I. M.; Fish, D.; Smid, J. In *Recent Adv. Anionic Polym., Proc. Int. Symp*; Hogen-Esch, T. E., Smid, J., Eds.; Elsevier: New York, 1986, p 451.
(26) Long, T. E.; DePorter, C. D.; Patel, N.; Dwight, D. W.; Wilkes, G. L.; McGrath, J. E. *Polym. Prepr. (Am. Chem. Soc., Div. Polym. Chem.)* **1987**, *28*(2), 214.
(27) Storey, R. F.; George, S. E. *Polym. Mat. Sci. Eng.* **1988**, *58*, 985.
(28) Stadler, R.; Moeller, M.; Burgert, J.; Omeis, J.; de Lucca Freitas, L. In *Integration of Fundamental Polymer Science and Technology II*; Kleintjens, L. A., Lemstra, P. J., Eds.; Elsevier Applied Science: London, 1987; p 94.
(29) Gauthier, S.; Eisenberg, A. *Macromolecules* **1987**, *20*, 760.
(30) Dubuisson, J. M.; Dauvergne, J. M.; Depautex, C.; Vachette, P.; Williams, C. E. *Nucl. Instr. Meth. Phys. Res.* **1986**, *A246*, 636.
(31) de Gennes, P.-G. *Scaling Concept in Polymer Physics*; Cornell University Press: Ithaca, NY, 1979.
(32) Hashimoto, T.; Fujimura, M.; Kawai, H. *Macromolecules* **1980**, *13*, 1660.

Variable-Density Model of Polymer Melt Surfaces: Structure and Surface Tension

Doros N. Theodorou

Department of Chemical Engineering, University of California, Berkeley, and Center for Advanced Materials, Lawrence Berkeley Laboratory, Berkeley, California 94720.
Received December 27, 1988; Revised Manuscript Received April 24, 1989

ABSTRACT: A variable-density lattice model is developed for the prediction of structure and thermodynamic properties at free polymer melt surfaces and polymer melt/solid interfaces. The model combines ideas from Scheutjens and Fleer's interfacial theory of polymer solutions and from the equation of state theory of Sanchez and Lacombe. Its derivation is based on the thermodynamic concept of availability. The model is implemented to study free surfaces of macromolecular liquids. The variation of surface tension with chain length and temperature is accurately predicted. The relative magnitude of enthalpic and entropic contributions to surface tension is correctly assessed. Surface tension values, obtained by using the Sanchez–Lacombe equation of state parameters, are lower than experimental, mainly because long-range segment–segment interactions are not accounted for in the lattice model. The density profile at a free surface is sigmoidal and approximately 15 Å thick for all chain lengths. Sparse, perpendicularly oriented chain tails protrude into the highly attenuated surface region. Chains are flattened immediately below this region. As one moves further into the melt, conformations narrow down to their asymptotic unperturbed characteristics, over a length roughly equal to the root mean squared end-to-end distance of chains.

1. Introduction

The surface and interfacial properties of polymers, in the condensed amorphous state, are important in a variety of technical areas. The role of polymers is becoming increasingly significant in manufacturing mechanical components with controlled friction and wear characteristics, in manipulating the wettability of surfaces by aqueous and organic fluids, and in developing new biocompatible materials. The science and technology of lubrication relies heavily on the interfacial behavior of polymers, as most lubricants are macromolecular liquids. The quality of products obtained through polymer-processing operations, such as extrusion and film blowing, is profoundly affected by surface-related dynamic phenomena (e.g., melt fracture[3]).

To judiciously select and efficiently design materials for these and similar applications, we need to understand the relationships between polymer chemical structure and macroscopically manifested interfacial properties at the molecular level. Adsorptive segment–solid interactions, or the lack thereof in polymer/gas systems, as well as entropic constraints at a phase boundary, cause the conformation of polymer chains to deviate from what it is in the bulk. Perturbations in local structure, in turn, govern thermodynamic, transport, mechanical, and optical properties in the interfacial region.

The adsorption of polymers from solution on solid surfaces has been studied in considerable detail. A concrete and particularly successful lattice model for this situation was developed by Scheutjens and Fleer.[1] Much

0024-9297/89/2222-4578$01.50/0

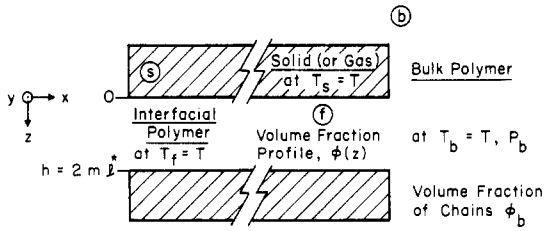

Figure 1. Model system considered in this work and definition of the solid (or gas), interfacial polymer, and bulk polymer phases.

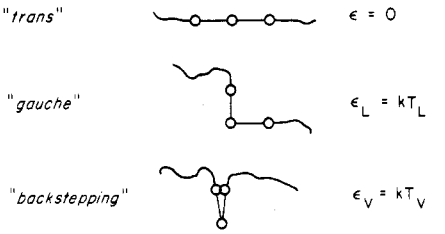

Figure 2. Lattice conformational states and their characteristic energies.

less attention has been devoted to the behavior of bulk polymers at interfaces, however. Previous theoretical approaches can be roughly divided into two categories: efforts to elucidate surface structure and efforts to predict surface tension. Weber and Helfand[4] considered the structure of an infinite molecular weight polymer melt near a nonadsorbing plane barrier. More recently, a Monte Carlo simulation of the free surface structure of a polymer melt was performed by Madden[5] using an efficient pseudokinetic algorithm to sample configuration space. As regards the prediction of surface tension, we mention here a successful treatment by Poser and Sanchez,[6] which combines the Cahn–Hilliard theory of nonuniform systems with a lattice-based equation of state, developed by Sanchez and Lacombe.[2] Despite these efforts, there exists today no unified theoretical approach that can both provide realistic estimates of polymer surface tension and a detailed, consistent picture of interfacial structure. Moreover, the solid/polymer interface problem is largely unexplored. A theory is needed that can explicitly incorporate segment/surface interactions and their effects on interfacial structure and properties.

We have recently introduced a simple, constant-density lattice model of the thermodynamics and structure of bulk homopolymers at interfaces.[7] Here we develop a more refined model that incorporates density variations in the interfacial region. Our intention is to complement the Poser–Sanchez theory[6] with a new approach that (a) takes full advantage of the information content of the lattice model and invokes no continuum concepts foreign to a lattice representation; (b) is based on a rigorous thermodynamic analysis of the interfacial region that employs solely equation of state parameters; (c) provides a detailed picture of interfacial structure at the molecular level, in addition to observable thermodynamic properties; (d) is applicable to polymer/solid interfaces as well as to free polymer surfaces.

The material presented in this paper is organized under three headings. Section 2 is a brief outline of the theoretical development, which applies to both polymer melt surfaces and polymer melt/solid interfaces. In Section 3, we use the theory to explore the free surface structure and tension of alkanes and polymer melts. Some important points are summarized in Section 4.

2. Theory

The system examined in this work is a monodisperse homopolymer melt, lying between two flat surfaces, in contact with unconstrained bulk polymer (Figure 1). Three phases are distinguished: the solid (nonpolymer) phase s, the interfacial polymer phase f, and the bulk polymer b. For studying free polymer surfaces, the solid phase is substituted by an energetically neutral gas phase. In the latter case, the planar polymer film f is inherently metastable; in the absence of external fields, it would break and incoporate itself into the bulk polymer surrounding it, to minimize surface area. Nevertheless, if the film thickness is large enough, its middle region is indistinguishable from bulk polymer, and the model becomes representative of a single polymer surface.

Our approach rests on the following assumptions:

1. The solid surfaces are molecularly smooth and energetically homogeneous. Their extent in the x- and y-directions is effectively infinite, and end effects are neglected. The solid phase is impenetrable by polymer and completely incompressible.

2. The polymer is composed of monodisperse, linear chains. In both phases f and b, the polymer is represented as a simple cubic lattice, whose sites are filled by chain segments (beads) and voids. The bulk polymer phase is infinite in extent. The density of the polymer phase can adjust to changes in temperature and pressure, as well as to the special energetic and entropic conditions prevailing at the interface, through changes in the local concentration of voids.

3. In laying down chains in the model polymer lattice, the Bragg–Williams approximation of random mixing is used to account for excluded volume effects in a layerwise fashion.[1] Configurational entropy is obtained by using the simple "Flory"[2] (or large coordination limit) approximation. A layerwise mean field approximation is also used in calculating the energy of segment–segment interactions and intramolecular energy.

Adsorptive interactions are active only between segments adjacent to a solid surface and sites on that surface. A potential energy w_{AS} is contributed by each adsorbed segment. The molecular picture we invoke is consistent with that of Sanchez and Lacombe.[2] The nature of the fluid is expressed through three parameters: the chain length r, the attractive energy between adjacent segments w_{AA}, and the segmental volume v^* or, equivalently, by r, T^*, and P^*, where

$$T^* = -z\frac{w_{AA}}{2k}; \quad P^* = \frac{RT^*}{v^*} \tag{1}$$

We will be using the Sanchez–Lacombe parameters in all that follows. In addition, conformational contributions to the intramolecular energy will be considered in some calculations (see Figure 2). For symmetry with eq 1, we introduce the temperature T_s^* in lieu of the energy w_{AS}:

$$T_s^* = -\frac{w_{AS}}{k} \tag{2}$$

Developing a model for our system amounts to deriving an appropriate expression for "free energy" and minimizing this free energy function to impose the conditions of equilibrium.

Since density can vary in the polymer phase, pressure appears as a variable. Let P_b be the pressure in the bulk polymer phase. Pressure in the film of Figure 1 is anisotropic.[8-10] The question thus arises, what pressure should one use in defining a "free energy" for the system? The answer is provided in Modell and Reid's superb textbook of thermodynamics.[11] By consideration of a system containing interfaces, at equilibrium with a constant-tem-

perature and constant-pressure reservoir, it is shown there that the appropriate "free energy" quantity is the *availability* $\hat{\Upsilon}$, a generalized Gibbs energy, defined in each phase by the temperature and pressure of the reservoirs. In our system, the bulk polymer phase plays the role of a constant temperature and pressure reservoir, at T and P_b. Then[12]

$$\hat{\Upsilon}_\alpha \equiv \hat{U}_\alpha + P_b\hat{V}_\alpha - T\hat{S}_\alpha \quad (\alpha = s, f, b) \tag{3}$$

Our first objective is to develop expressions for the availability of the interfacial polymer ($\hat{\Upsilon}_f$) and of the bulk polymer ($\hat{\Upsilon}_b$) by a statistical mechanical analysis of the lattice model.

Availability of the Interfacial Film. An expression for $\hat{\Upsilon}_f$ can be obtained by using the formalism of the isothermal–isobaric ensemble to describe a system of n_f chains in the interfacial region, together with a maximum term approximation for the partition function. Detailed derivations have been presented elsewhere.[13] Only a brief outline of the theoretical formulation is given here. In the notation of ref 7, the distribution of conformations in the interfacial region is found to obey the form

$$n_c = \exp(-\xi + r \ln L)\{\omega_c \exp(-\epsilon_c/kT)\} \exp[\sum_{i=1}^{2m} r_{i,c}\{\ln (1 - \varphi_i) + 2\chi\langle\varphi_i\rangle + (\delta_{i,1} + \delta_{i,2m})(\lambda_1\chi + \chi_s)\}] \tag{4}$$

where φ_i is the volume fraction of polymer in layer i and the "site volume fractions" $\langle\varphi_i\rangle$ are defined as in ref 1. The interaction parameters χ and χ_s are dimensionless measures of cohesive and adhesive interactions:

$$\chi = -\frac{zw_{AA}}{2kT} = \frac{T^*}{T}$$

$$\chi_s = -\frac{\lambda_1 z}{kT}\left(w_{AS} - \frac{1}{2}w_{AA}\right) = \lambda_1\left(\frac{zT_s^* - T^*}{T}\right) \tag{5}$$

The quantity ϵ_c denotes conformational energy, and ξ is a Lagrange multiplier, associated with the constraint that the sum of all n_c must equal n_f. The prefactor $\exp[-\xi + r \ln L]$ in the distribution, eq 4, is conformation-independent. The factor $\omega_c \exp(-\epsilon_c/(kT))$ is purely intramolecular, i.e., proportional to the probability of occurrence of conformation c in the isolated unperturbed state. The last factor can readily be cast into the form of a product over all layers, to which the successive segments of a chain belong under the conformation c.[1,7] It incorporates all contributions from inter- and intramolecular long-range effects and from chain–surface interactions. The availability of the interfacial polymer is calculated as[13]

$$(1/kT)\hat{\Upsilon}_f(T,P_b,n_f,\hat{a},h) = n_f\{(r-1)(1 - \ln z) + [-\xi + (r-1)\ln L]\} + 2L\sum_{i=1}^{m}\{\chi\varphi_i\langle\varphi_i\rangle + \ln(1-\varphi_i)\} + 2mL(P_bv^*/RT) \tag{6}$$

The microscopic degree of freedom L (equivalently, the surface area $\hat{a}$ wetted by the n_f interfacial chains on each plate) is included among the arguments of $\hat{\Upsilon}_f$. This degree of freedom is to be fixed by imposing the condition of minimal total availability. At equilibrium, only four of the five arguments of $\hat{\Upsilon}_f$ in eq 6 are independent.

Conformation Propagation and Segment Balance Equations. The simple product form of the distribution of conformations in the film region, eq 4, permits the self-consistent determination of the volume fraction profile $\{\varphi_i\}$, given the factor $-\xi + (r-1)\ln L$ and the molecular characteristics of the system. It is convenient to introduce the "free segment probabilities"[1] P_i, defined by

$$\ln P_i = \ln(1-\varphi_i) + 2\chi\langle\varphi_i\rangle + (\delta_{i,1} + \delta_{i,2m})(\chi_s + \lambda_1\chi) \tag{7}$$

"End segment probabilities"[1] $P(i,s)$, proportional to the likelihood that a subchain s segments long (starting anywhere in the lattice) has its sth segment in layer i, are similarly introduced. In the absence of conformational contributions to intramolecular energy, the quantitites $P(i,s)$ can be obtained from the $\{P_i\}$ profile via the recursive eq 35 of ref 7. The inclusion of chain stiffness can be dealt with through a more elaborate, second-order recursive "conformation propagation" scheme, following the ideas introduced by Di Marzio and Rubin[14] and Leermakers et al.[15] Considering a chain as a sum of two subchains, sharing a common segment, the following self-consistency "segment balance" conditions are derived:

$$\varphi_i = \exp[-\xi + (r-1)\ln L]\frac{1}{P_i}\sum_{s=1}^{r}P(i,s)P(i,r-s+1)Y(i,s) \quad (1 \le i \le m) \tag{8}$$

The coefficients $Y(i,s)$ deal with the conformational energy contribution from the junction between the two subchains; they are functions of the end segment probability matrix.[13] For a given value of the prefactor $\exp[-\xi + (r-1)\ln L]$, the segment balance eq 8, together with the recursive conformation propagation equations and the definitions, eq 7, comprise a nonlinear system that can be solved for the m volume fractions φ_i, $1 \le i \le m$. Thus, closure of the model amounts to determining the quantity $-\xi + (r-1)\ln L$, an intensive property of the interfacial polymer.

Availability of the Bulk Polymer. An expression for the availability of the bulk polymer can be derived within the framework of the isothermal–isobaric ensemble, following Sanchez and Lacombe.[2] For a "flexibility parameter" of z^{r-1} (backstepping allowed) and a "symmetry number" of 1, the availability of n_b chains in a bulk phase at T and P_b, where the volume fraction of polymer is φ_b, is

$$\frac{1}{kT}\hat{\Upsilon}_b(T,P_b,n_b,\varphi_b) = n_b\left\{(r-1)(1-\ln z) - \ln r - r\varphi_b\chi + r\frac{1-\varphi_b}{\varphi_b}\ln(1-\varphi_b) + \ln\varphi_b + \frac{P_bv^*}{RT}\frac{r}{\varphi_b} - (r-2)\ln(\lambda_1 + \lambda_0\tau_L + \lambda_1\tau_V)\right\} \tag{9}$$

The last term in braces in eq 9 is the contribution to free energy due to intramolecular stiffness; τ_L and τ_V are Boltzmann factors associated with the penalty of a gauche (L) or a "backstepping" (V) placement of a pair of consecutive bonds, relative to trans[13] (see Figure 2). The separation of intermolecular and excluded volume from short-range intramolecular contributions to the availability in eq 9 stems from invoking the "random coil hypothesis" in the bulk.

Model Closure: Full Equilibrium. It remains to impose the condition of stable thermodynamic equilibrium between phases s, f, and b. We consider the thermodynamic system of Figure 3. This consists of equal and opposite portions of the two slabs of phase s at temperature T, each of surface area $\hat{a}$ and each containing n_s/N_L mol of solid or gas; of the interfacial polymer in between (n_f/N_L mol) at temperature T; and of a quantity of the surrounding bulk polymer (n_b/N_L mol) at temperature T and pressure P_b. The total polymer in the system

$$n = n_f + n_b = \text{const} \tag{10}$$

is fixed, as is n_s. The quantitites n_f and n_b are not fixed a priori; the polymer is allowed to distribute itself between

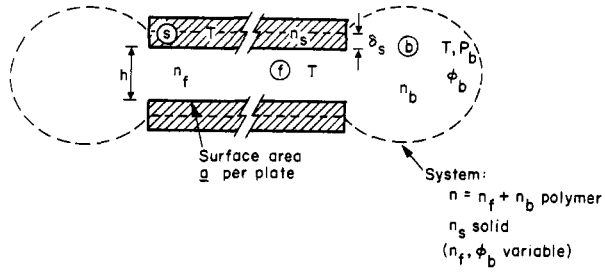

Figure 3. Selection of the thermodynamic system for equilibrium analysis.

the film phase and the bulk according to the requirements of equilibrium. The infinitely extending (assumption 2) bulk polymer phase b acts as a heat (constant T), work (constant P_b), and mass (constant chemical potential) reservoir for the interfacial polymer f. The film thickness is kept constant and equal to h. The control surface of Figure 3 intersects each plate along a plane, at which properties are indistinguishable from those of a bulk s phase.

Using eq 6 and 9, we can write the total availability of our thermodynamic system as

$$\hat{\Upsilon}(T,P_b,n,n_s,\hat{a},h;n_f,\varphi_b) = \hat{\Upsilon}_f(T,P_b,n_f,\hat{a},h) + \hat{\Upsilon}_b(T,P_b,n-n_f,\varphi_b) + \hat{\Upsilon}_s(T,P_b,n_s,\hat{a},\delta_s) = n_f\Upsilon_f(T,P_b,(n_f/\hat{a}),h) + (n-n_f)\Upsilon_b(T,P_b,\varphi_b) + \hat{\Upsilon}_s(T,P_b,n_s,\hat{a},\delta_s) \quad (11)$$

In eq 11 it has been recognized that the intensive quantity Υ_f can only depend on n_f and $\hat{a}$ through the intensive ratio $n_f/\hat{a}$. By assumption 1, the thermodynamics of phase s is completely decoupled from that of the polymer (incompressible solid or highly attenuated gas); T, P_b, n_s, $\hat{a}$ and δ_s will be related exactly as they would be in the absence of polymer. The total amounts of all components in the thermodynamic system of Figure 3 are constant, and the system is capable of interacting with a constant temperature and pressure reservoir. At equilibrium,[11] $\hat{\Upsilon}$ must be at a minimum with respect to (a) the amount of polymer between the plates n_f and (b) the volume fraction of polymer in the bulk phase φ_b.

Condition b leads directly to the Sanchez–Lacombe equation of state for the bulk polymer:[2,13,16]

$$\frac{P_b v^*}{RT} + \left(1 - \frac{1}{r}\right)\varphi_b + \ln(1-\varphi_b) + \chi\varphi_b^2 = 0 \quad (12)$$

Condition a is equivalent to

$$\hat{a}\left.\frac{\partial\hat{\Upsilon}_f}{\partial\hat{a}}\right|_{T,P_b,n_f,h} = n_f(\Upsilon_f - \Upsilon_b) \quad (13)$$

By use of eq 6 and 9, it can be cast into the form

$$-\xi + (r-1)\ln L = \ln(\varphi_b/r) - 2r\chi\varphi_b - r\ln(1-\varphi_b) - (r-2)\ln(\lambda_1 + \lambda_0\tau_L + \lambda_1\tau_V) \quad (14)$$

Equations 12 and 14 provide closure to our full equilibrium model. For a given temperature T and pressure P_b in the bulk phase, the volume fraction φ_b is determined by solving eq 12. The factor $-\xi + (r-1)\ln L$ is then immediately calculable from eq 14. Knowing this factor, we can obtain the volume fraction profile $\{\varphi_i\}$ in the interfacial region by the conformation propagation and segment balance equations, as described above. Furthermore, molar availabilities in the interfacial region are obtainable through eq 6 and 9. It should be pointed out that, in the absence of chain stiffness, our model is analogous to the original solution model of Scheutjens and Fleer,[1] with voids playing the role of solvent molecules and with the bulk volume fraction fixed by the Sanchez–Lacombe equation of state.[13]

Surface Tension and Adhesion Tension. In the system of Figure 3, we *define* interfacial tension γ in terms of the difference between the total availability of phases s, f, and b and the availability that the same amount of matter contained in the system would possess, if it belonged entirely to bulk s and polymer phases under the ambient conditions T and P_b:

$$2\gamma\hat{a} = n_f\Upsilon_f(T,P_b,h) + n_b\Upsilon_b(T,P_b) + n_s\Upsilon_s(T,P_b,\delta_s) - n_f\Upsilon_b(T,P_b) - n_b\Upsilon_b(T,P_b) - n_s\Upsilon_{sb}(T,P_b) = n_f[\Upsilon_f(T,P_b,h) - \Upsilon_b(T,P_b)] + n_s[\Upsilon_s(T,P_b,\delta_s) - \Upsilon_{sb}(T,P_b)] \quad (15)$$

The factor of 2 in eq 15 accounts for the presence of two f/s interfaces. The subscript sb denotes a bulk s phase of infinite extent in all three directions.

Consider now the system depicted in Figure 3 with all polymer in phases f and b replaced by vacuum. By assumption 1, the s phase in this new, vacuum-filled system will have exactly the same surface area $\hat{a}$ and the same molar availability Υ_s as in the original system. By definition, then, the difference $\Upsilon_s(T,P_b,\delta_s) - \Upsilon_{sb}(T,P_b)$ is related to the surface tension of pure s (against vacuum) by

$$2\gamma_s\hat{a} = n_s[\Upsilon_s(T,P_b,\delta_s) - \Upsilon_{sb}(T,P_b)] \quad (16)$$

Combining eq 15 and 16, we obtain

$$2(\gamma - \gamma_s)\hat{a} = n_f[\Upsilon_f(T,P_b,h) - \Upsilon_b(T,P_b)] \quad (17)$$

In solid/fluid systems, the quantity $-(\gamma - \gamma_s)$ is sometimes referred to as the "*adhesion tension*".[17] If the s phase is a solid, eq 17 provides a route for obtaining the adhesion tension from fundamental molecular information. If the s phase is a gas, then $\gamma_s = 0$, and γ on the left-hand side of eq 17 gives the *surface tension of the pure polymer*. It can be shown[13] that our definition of the adhesion tension in terms of availability is consistent with definitions used in previous theoretical work.[10,18]

Combining eq 17, 6, and 9, we obtain the following expression for the adhesion (surface) tension at a polymer/solid interface (free polymer surface) in terms of the volume fraction profile $\{\varphi_i\}$:

$$\gamma - \gamma_s = \frac{RT}{a^*}\left\{m\left(\frac{P_b v^*}{RT}\right) + \sum_{i=1}^{m}\left[\left(1-\frac{1}{r}\right)\varphi_i + \ln(1-\varphi_i) + \chi\varphi_i\langle\varphi_i\rangle\right]\right\} \quad (18)$$

By combining eq 18 and eq 12, one is led to an expression for $\gamma - \gamma_s$ that is identical with the surface tension expression of Scheutjens and Fleer for polymer solutions (eq 23 of ref 1 (1985)).

Interesting analogies exist between our lattice model and continuum approaches to the surface behavior of polymeric liquids. In the continuum limit, the sum in eq 18 reduces to an integral over half the volume of the f phase. The term $\chi\varphi_i\langle\varphi_i\rangle$ gives rise to a "nonlocal" contribution of the form $\chi\varphi^2 + \lambda_1\chi(l^*)^2\varphi\nabla^2\varphi$. The set of conformation propagation equations becomes a partial differential "diffusion and reaction" equation in the reduced end segment probability $p(z,t)$. Also, the set of segment balance equations reduces to an integral self-consistency relation between $\varphi(z)$ and $p(z,t)$.[19,20] In the limit of very long chains, this integrodifferential system can be used to express $\nabla^2\varphi$ in terms of φ and the squared gradient $(\nabla\varphi)^2$. The right-hand side of eq 18 is thus cast into an integral involving $(\nabla\varphi)^2$. The coefficient in $(\nabla\varphi)^2$ in this expression for surface

tension involves "enthalpic" terms, reminiscent of the Poser–Sanchez[6] theory; additionally, it contains "entropic" terms due to the conformational restriction of chains at the surface, which are analogous to the entropic correction proposed by Rabin.[21]

Another interesting connection can be made between eq 18 and the "mechanical definition" of surface tension.[8,10,22] Consider the model system with s = gas phase, as the number of layers $m \to \infty$. From eq 18, we can write the polymer surface tension as

$$\gamma = \frac{RT}{a^*}\sum_{i=1}^{m}(P_b - P_{T,i})\frac{v^*}{RT} = \sum_{i=1}^{m}(P_b - P_{T,i})l^* \qquad (19)$$

where $P_{T,i}$ is defined by

$$\frac{P_{T,i}v^*}{RT} = -\left(1 - \frac{1}{r}\right)\varphi_i - \ln(1 - \varphi_i) - \chi\varphi_i\langle\varphi_i\rangle \qquad (20)$$

If we accept that the Sanchez–Lacombe equation of state is followed *locally within the interfacial region*, then we can identify $P_{T,i}$ as the component of pressure in the *transverse* (x or y) direction; in this direction, the density of the system is "smeared", and volume fluctuations are not constrained by the layerwise discretization of the lattice. Taking eq 19 to the continuum limit $m \to \infty$

$$\gamma = \int_{-\infty}^{\infty}[P_b - P_T(z)]\,dz \qquad (21)$$

where the limit $+\infty$ corresponds to the unconstrained bulk polymer and the limit $-\infty$ to the bulk gas phase, in which no polymer is present. Equation 21 constitutes the "mechanical definition" of surface tension and points to the internal consistency of our variable-density approach.

Structural Features. The molecular detail of our lattice model allows obtaining a variety of structural features from its solution. Techniques for calculating some of these features, developed in ref 7, can readily be extended to the variable-density case.[13] Structural features to be studied in the following include the bond order parameter S_i, the average width n_{si} of a chain passing through layer i, and the volume fraction $\varphi_i(s)$ of segments of order s in the film.

3. Modeling the Free Surface of Macromolecular Liquids

Chain-Length Dependence of Surface Tension. Our purpose in this section is to apply the theoretical development outlined in section 2 to free surfaces of macromolecular liquids. In modeling a free surface, the semiinfinite nonpolymeric domains s represent gaseous phases at T and P_b. The volatility of the liquid is neglected. This is an excellent approximation for high molecular weight polymer melts. In short-chain liquids, a vapor exists in the bulk gas phase. As the density of this vapor will ordinarily be on the order of 10^3 times lower than the bulk liquid density, its effects on surface structure and tension are neglected. Density is assumed to drop to exactly zero as one traverses the surface in the z-direction. The z value at which this happens defines the location of the (conceptual) planes separating phase f from the s phases. Note that a more elaborate formulation of the free surface problem, including the vapor phase in equilibrium with the liquid, would well be possible within the framework of our lattice model.

By definition, a free liquid surface is characterized by $T_s^* = 0$. The free surface problem in a melt of freely jointed chains can thus be formulated exclusively in terms of the three Sanchez–Lacombe equation of state parameters r, T^*, and P^*.

To test the performance of our model in predicting the chain-length dependence of surface tension, we applied it to the homologous series of normal alkanes. Values of the parameters r, T^*, and P^*, chosen so as to fit experimental density and vapor pressure data, are provided in ref 2. Note that the chain length r does not correspond exactly, and is not even proportional, to the actual number of carbon atoms in a molecule; limitations of the lattice representation have been absorbed into the parameters r, T^*, and P^*. Note, also, that the Sanchez–Lacombe r can assume noninteger values; on the other hand, our interfacial lattice formulation demands an integer r. To reconcile this difference, two runs were performed for each of the cases studied here, using as r the two integers bracketing the Sanchez–Lacombe value. Thermodynamic properties were calculated by linear interpolation between the results of these two runs. A single-variable Newton–Raphson analysis was used for the numerical solution of the equation of state, eq 12, for φ_b. The system of interfacial equations was solved for the $\{\varphi_i\}$ profile by straightforward multivariate Newton–Raphson analysis, based on an analytical Jacobian.[7] The amount of polymer per unit area in the f film is related to the average volume fraction $\bar{\varphi}$ in the film by

$$\bar{\varphi} = \frac{1}{m}\sum_{i=1}^{m}\varphi_i = \frac{n_f}{\hat{a}}\left(\frac{1}{2}\,\frac{ra^*}{mN_L}\right) \qquad (22)$$

The strong nonlinearity of the free surface problem is manifested in a multiplicity of solutions. For given T, P_b, r, T^*, P^* and m, there are several $\{\varphi_i\}$ profiles that satisfy the model equations, each corresponding to different $\bar{\varphi}$ and γ. For n-hexane, for example, one can use $r = 8$, $T^* = 476$ K, $P^* = 298$ MPa, $T_L = T_V = 0$, and $m = 20$. At $T = 293$ K and $P_b = 1$ bar, one locates solutions with $\bar{\varphi} = 0.802$ ($\gamma = 11.127$ mN/m), $\bar{\varphi} = 0.765$ ($\gamma = 10.872$ mN/m), $\bar{\varphi} = 0.723$ ($\gamma = 10.856$ mN/m), $\varphi = 0.680$ ($\gamma = 10.873$ mN/m), $\bar{\varphi} = 0.637$ ($\gamma = 10.894$ mN/m), and $\bar{\varphi} = 0.594$ ($\gamma = 10.915$ mN/m). In all these solutions, the volume fraction φ_i becomes indistinguishable from φ_b in the middle region of the polymer layer. In the vicinity of the gas phase, the volume fraction profiles differ among the various solutions; this difference, however, is much more a difference in position than in shape. The profiles are, to a good approximation, superposable by translations along the z axis. This is reflected in the small differences between the γ values characteristic of the different solutions. In view of this, the observed multiplicity of solutions appears to be due to the artificial discretization imposed by the lattice model, rather than to point to the existence of physically different metastable surface states. All results reported here are based on the stablest among the multiple solutions; this is the solution of lowest total availability, or, equivalently, of lowest surface tension. A zero-order continuation scheme in r, T^*, and P^* was used for the numerical solution. The $\{\varphi_i\}$ profiles of higher homologues were obtained from that of n-hexane at the same T and P_b, through a series of "chemical transformations" from each homologue to the next one, using the last determined volume fraction profile as an initial guess.

Model predictions for the surface tension of alkanes at 20 °C and 1 bar, obtained by using a freely jointed chain representation, based solely on the Sanchez–Lacombe parameters, are plotted against experimental values in Figure 4 (open circles). Two observations can be made on the basis of these results:

(a) A linear relationship exists between predicted and experimental surface tensions. Some deviation from the least-squares line is observed in the case of hexane and

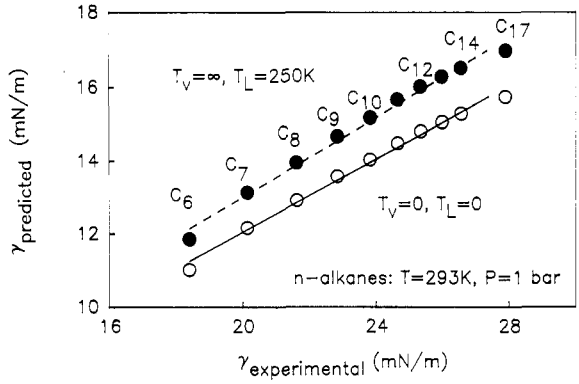

Figure 4. Predicted surface tensions plotted against experimental values in the homologous series of normal alkanes, at T = 20 °C and P_b = 1 bar. Open circles: variable-density model with no intramolecular energy contribution. Filled circles: variable-density model with T_L = 250 K and T_V = ∞. The parameters r, T^*, and P^* recommended in ref 2 (1976, Table I; 1978, Table I) were used in both cases. Experimental data are from ref 23, Table 51.4. Least-squares lines have been drawn through the points.

Table I
Temperature Dependence of Surface Tension of Linear Polyethylene at 1 bar

temp t, °C	exptl[a] γ, mN/m	predicted[b] γ, mN/m	$-(T/\gamma)\partial\gamma/\partial T$ expt[c]	$-(T/\gamma)\partial\gamma/\partial T$ model[c]
136	28.85	19.68		
146	28.49	19.32	0.84	0.79
155	27.77	18.99	0.89	0.83
165	27.33	18.61	1.01	0.88
173	26.64	18.31	1.27	0.92
182	26.04	17.97	0.81	0.97
192	25.76	17.59		

[a] Read from ref 25, Figure 2. Measurements reported in that reference were performed by the pendant drop method on samples of linear polyethylene (Alathon 7050, Du Pont) of melt index 20, containing approximately 0.2 methyl groups per 100 carbon atoms (estimated[26] weight-average molecular weight 38 000). [b] Variable-density model calculations, obtained by using the Sanchez–Lacombe parameters $r = 1.22r_u$, T^* = 649 K, and P^* = 426 MPa for linear polyethylene (ref 2: 1978, Table II; 1977; Table I) and neglecting chain stiffness ($T_L = T_V = 0$). In defining r_u, a skeletal methylene ($-CH_2-$) is used as the monomer unit. All calculations were performed on a monodisperse melt of r_u = 100-unit chains. [c] Estimated by finite differences from entries in the three first columns of Table I as $-(T/\gamma)(\partial\gamma/\partial T)|_{P_b} = [(t_i + 273.15)/(t_{i+1} - t_{i-1})][(\gamma_{i-1} - \gamma_{i+1})/\gamma_i]$ where i = 2 (1) 6 is the row index in the table.

heptadecane. Note that liquid heptadecane is metastable at 20 °C; the experimental value of γ used in Figure 4 is an extrapolation. The linearity between theoretical and experimental γ values indicates that the scaling of surface tension with molecular weight is correctly predicted. Surface tensions within a homologous series of macromolecular fluids have been successfully correlated[24] as

$$\gamma = \gamma_\infty - K/M^{2/3} \tag{23}$$

The experimental and predicted alkane surface tensions of Figure 4 can be fitted with eq 23 with correlation coefficients of 0.998 and 0.996, respectively.

(b) Although the scaling of surface tension with molecular weight is captured correctly, the actual values of surface tension are underestimated by the model. Model predictions for alkanes are on the average 41% lower than the corresponding experimental values. The error is somewhat lower in the case of longer chain polymers (32% for linear polyethylene and 28% for poly(dimethylsiloxane), Tables I and II).

The question arises, why does a representation that fits bulk volumetric data[2] within 1% lead to an underestimation of surface tension? One possible reason could be that intramolecular conformational energy (chain stiffness) was neglected in the calculations. To test this hypothesis, we repeated the model calculations on normal alkanes, using a characteristic temperature for *gauche* placement equal to T_L = 250 K and a characteristic temperature for *backstepping* equal to T_V = ∞. In this case, the system of model equations[13] was solved by Brown's method,[27] without analytical derivatives. The value of T_L is consistent with the experimental difference[28] of roughly 0.5 kcal/mol between trans and gauche minima. Surface tensions, predicted in the presence of chain stiffness, are plotted in Figure 4 as filled circles. They are 8% higher than the corresponding predictions for freely jointed chains. This rather small improvement indicates that neglecting conformational energy is not the primary reason for underestimating surface tension. The primary reason lies in the modeling of segment–segment interactions. In our lattice representation, an infinite-range van der Waals type nonbonded interaction is substituted by a square-well potential, active only between nearest-neighbor segments. In Sanchez and Lacombe's equation of state work, this substitution is compensated for by appropriate fitting of parameters. These parameters, however, are no longer satisfactory in an intrinsically inhomogeneous and anisotropic system, such as the surface. Here, omission of potential tails leads to an underestimation of surface tension. At this point, one could revise model parameters (mainly the characteristic temperature T^*) so as to enforce agreement with experiment. Interestingly, such a revision has been undertaken in the surface tension model of Poser and Sanchez.[6] In order to use the Cahn–Hilliard formalism, these authors substitute the original lattice square-well potential with a Sutherland-type potential, which yields the same cohesive energy density in the bulk; the attractive part of this potential consists of a smooth, inverse-power expression. The exponent in that expression is effectively treated as a fourth adjustable parameter by Poser and Sanchez, to ensure accurate estimates of surface tension. Although such a revision of parameters is possible within the framework of our variable-density model, we chose not to implement it here, as it is essentially foreign to the lattice picture we invoke. Also, since accounting for intramolecular energy effects, at a substantial computational cost, does not alter our predictions significantly, we

Table II
Temperature Dependence of Surface Tension of Poly(dimethylsiloxane) at 1 bar

temp t, °C	exptl[a] γ, mN/m	predicted[b] γ, mN/m	$-(T/\gamma)(\partial\gamma/\partial T)$ expt[c]	$-(T/\gamma)(\partial\gamma/\partial T)$ model[c]
30	19.79	14.19		
60	18.02	13.12	0.99	0.92
89	16.62	12.05	1.16	1.11
116	15.05	11.05	1.37	1.30
146	13.61	9.94	1.37	1.54
173	12.51	8.97		

[a] Read from ref 25, Figure 2. Measurements reported in that reference were performed by the pendant drop method on Dow Corning Silicone 200 fluids of viscosity 10^6 and 6×10^4 cSt (estimated[26] molecular weights 410 000 and 180 000, respectively). Surface tension results were identical between the two molecular weights, within the experimental error of ±0.3 mN/m. No information is given on sample polydispersity. [b] Variable-density model calculations, obtained by using the Sanchez–Lacombe parameters $r = 5.12r_u$, T^* = 476 K, and P^* = 302 MPa for poly(dimethylsiloxane) (ref 2: 1978, Table II; 1977, Table I) and neglecting chain stiffness ($T_L = T_V = 0$). In defining r_u, $-Si(CH_3)_2O-$ is used as the monomer unit. All calculations were performed on a monodisperse liquid of r_u = 50-unit chains. [c] See footnote c to Table I.

chose to set $T_L = T_V = 0$ in all subsequently reported calculations for long-chain systems. To use our lattice approach as a quantitative predictor of surface tension, one should apply correction factors of 1.70, 1.46, and 1.38 in the case of normal alkanes, polyethylene and poly(dimethylsiloxane), respectively.

A final point, worth mentioning here, is that the estimates of γ, obtained by our variable-density lattice approach, are coordination number dependent. If one introduces a hcp ($z = 12$) in place of a simple cubic ($z = 6$) lattice to represent hexane, keeping the values of r, T^*, and P^* constant, the predicted surface tension increases by 22%. Extrapolation to a lattice of infinite coordination number would give γ values close to the experimental values. Such an extrapolation is not implemented here. A simple cubic lattice is used in all calculations as the simplest possible model, whereby interfacial structure and thermodynamics can be investigated simultaneously and self-consistently.

Temperature Dependence of Surface Tension. An interesting aspect, that can readily be explored with our variable-density lattice approach is the temperature dependence of surface tension. This provides a measure of the relative significance of entropic and enthalpic contributions to surface thermodynamic properties.

By definition of the surface tension, we can express the differential of internal energy in the system f + b + s as[10]

$$d\hat{U} = G_b dn + T d\hat{S} - P_b d\hat{V} - (P_N - P_b)\hat{a} dh + 2\gamma d\hat{a} \tag{24}$$

Introducing the total availability $\hat{\Upsilon}$ as the second Legendre transform of $\hat{U}$ with respect to $\hat{S}$ and $\hat{V}$, and using a Maxwell relation on $d\hat{\Upsilon}$, we can write

$$\gamma = \gamma_{enthalpic} + \gamma_{entropic} \tag{25}$$

where

$$\gamma_{enthalpic} = \frac{1}{2} \left. \frac{\partial(\hat{U}+P_b\hat{V})}{\partial \hat{a}} \right|_{n,T,P_b,h} \tag{26}$$

$$\gamma_{entropic} = T \left. \frac{\partial \gamma}{\partial T} \right|_{n,P_b,h,\hat{a}} \tag{27}$$

At large enough separations h, which are of interest here, γ is an intensive property, dependent on T and P_b only, and representative of a single free fluid surface. Equation 27 is simplified to

$$\gamma_{entropic} = T \left. \frac{\partial \gamma}{\partial T} \right|_{P_b} \tag{28}$$

Observe that $\gamma_{entropic}$, as defined by eq 28, is an intrinsically negative quantity. We will use the dimensionless ratio

$$-\frac{\gamma_{entropic}}{\gamma} = -\frac{T}{\gamma} \left. \frac{\partial \gamma}{\partial T} \right|_{P_b} \tag{29}$$

as a measure of the entropic contribution to surface tension, relative to its total value. Note that this ratio is positive but not a priori constrained to take on values less than unity.

Surface tensions, predicted at various temperatures for a monodisperse, linear polyethylene of molecular weight 1400, are compared against experimental data in Table I. The molecular weight used in the calculations is lower than that of the experimental samples. Nevertheless, it is high enough for the reduced quantity $(T/\gamma)(\partial\gamma/\partial T)|_{P_b}$ to be practically molecular weight independent. The predicted values of γ are lower than experimental values by 32%, as discussed above. Nevertheless, the effect of temperature

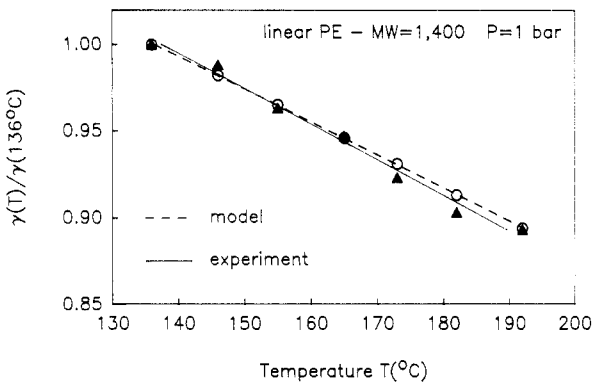

Figure 5. Temperature dependence of surface tension in linear polyethylene. Surface tension, reduced by its value at 136 °C, is plotted as a function of temperature. Open symbols: model predictions. Filled symbols: experimental measurements. The broken and solid lines have been drawn by linear regression through the predicted and experimental points, respectively. The figure is a graphical representation of the data in Table I.

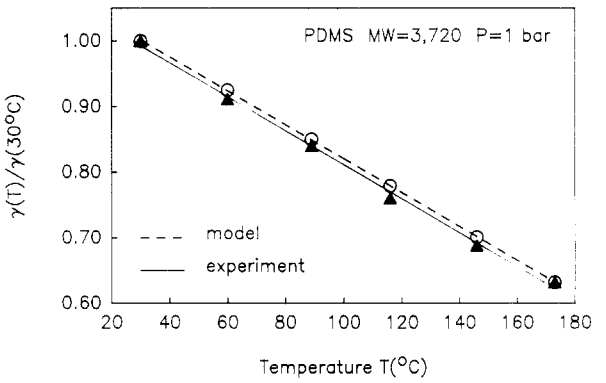

Figure 6. Temperature dependence of surface tension in poly(dimethylsiloxane). Surface tension, reduced by its value at 30 °C, is plotted as a function of temperature. Open symbols: model predictions. Filled symbols: experimental measurements. The figure is a graphical representation of the data in Table II.

on surface tension is very successfully predicted by the model. To demonstrate this, we reduce both theoretical and experimental surface tensions by their values at 136 °C and plot the ratios thus formed against temperature in Figure 5. The model and experimental curves coincide within the accuracy of the measurement. This implies that entropic contributions to surface tension are correctly assessed by the model. To test this hypothesis, we form the dimensionless entropic contribution $-(\gamma_{entropic}/\gamma)$ (eq 29) by finite differentiation of the second and third columns of Table I. Results are listed in the fourth and fifth columns of the same table. Within the accuracy of the data, experimental and model values for the relative significance of entropic effects are in excellent agreement. Note that the contribution of entropy to γ increases with increasing temperature.

The temperature dependence of surface tension in poly(dimethylsiloxane) is examined in Table II, along the same lines. In this case, the better quality of the experimental data facilitates comparison between theory and experiment. Surface tension, reduced by its value at 30 °C, is plotted in Figure 6. The experimental and model lines in that figure are practically indistinguishable. Experimental and model estimates of the entropic contribution to surface tension, listed in the last two columns of Table II, are in excellent agreement.

The general conclusion from these calculations is that although our variable-density model underestimates surface tension, it correctly captures the relative significance

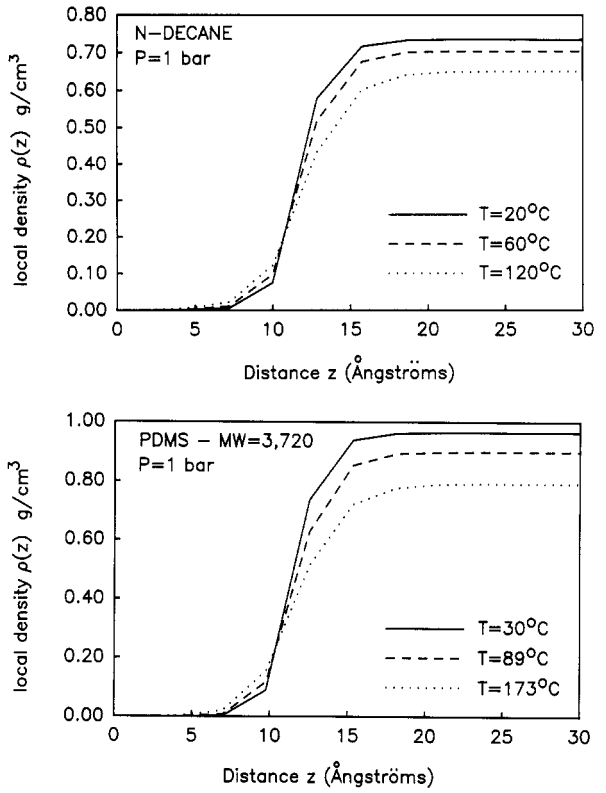

Figure 7. Density profiles at the free surface of macromolecular liquids, as predicted by the variable-density model. (a) Normal decane with $r = 12$, $T_L = 250$ K, $T_V = \infty$. (b) Poly(dimethylsiloxane) liquid, of molecular weight 3720, with $r = 256$, $T_L = T_V = 0$. The Sanchez–Lacombe parameters T^* and P^* have been used in all calculations.

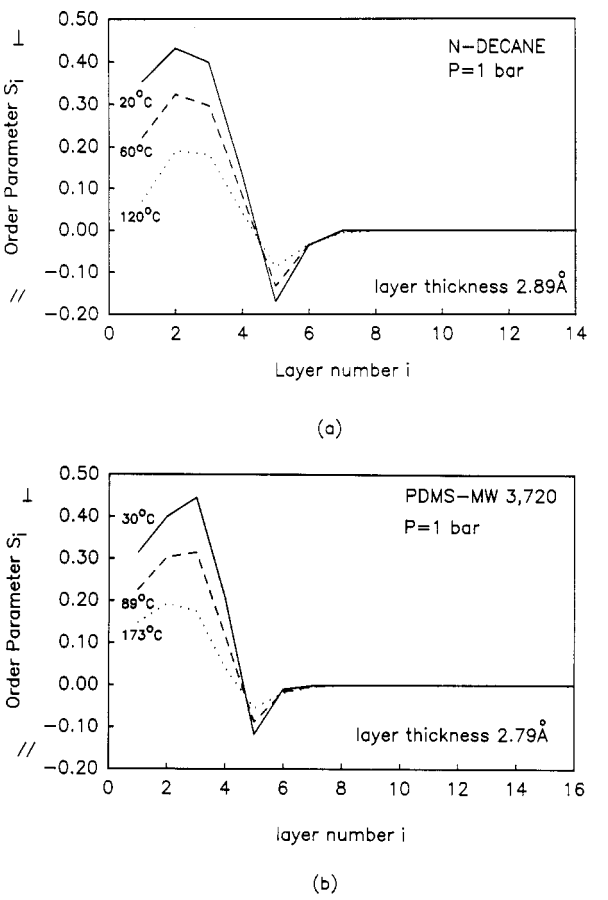

Figure 8. Bond order parameter profiles S_i at the free surface of (a) normal decane and (b) a 50-unit poly(dimethylsiloxane) of molecular weight 3720. See also caption of Figure 7.

of its enthalpic and entropic components. Interestingly, the entropic contribution to surface tension in long-chain liquids is less successfully predicted by the Poser–Sanchez theory,[6] although that theory does a better job than our lattice model in fitting room temperature surface tension values. This is because the Poser–Sanchez approach is purely a density approach. It does not explicitly take into account the constraints imposed on conformations at a surface. This leads to a substantial overestimation of surface entropy.[21] On the contrary, our lattice model incorpates a detailed consideration of the distribution of conformations in the surface region.

Density Distribution. We present here results on surface structure, obtained for two representative systems: (a) normal decane, modeled by using $r = 12$ and the Sanchez–Lacombe T^* and P^*, with explicit consideration of conformational energy ($T_L = 250$ K, $T_V = \infty$); (b) a monodisperse poly(dimethylsiloxane) liquid of molecular weight 3720, modeled exactly as described in Table II, with $T_L = T_V = 0$. By comparing these two systems, we will probe the effects of chain length on surface structure.

In Figure 7, local density profiles

$$\rho(z) = \rho_i = \varphi_i(M/rv^*) \tag{30}$$

are plotted as a function of vertical position

$$z = \left(i - \frac{1}{2}\right)l^* \tag{31}$$

The plane beyond which no chain segments are detected is used to define the origin for measuring z.

Density profiles are sigmoidal, rising from a value of practically zero to their asymptotic bulk value over a distance on the order of 15 Å. The thickness of the surface region, over which density variations are observed, is quite insensitive to chain length. Density distributions become more diffuse with increasing temperature. The profiles in Figure 7 are in general agreement with those predicted with the theory of Poser and Sanchez[6] as well as with a recent Monte Carlo simulation of a free melt surface.[5]

Bond Orientation. As a measure of orientation effects induced by the surface, we introduce the bond order parameter[7] in layer i

$$S_i = \frac{1}{2}\left(3\frac{n_{bi-1}^N + n_{bi}^N}{n_{bi-1}^N + n_{bi}^N + 2n_{bi}^L} - 1\right) \tag{32}$$

In eq 32, n_{bi}^N (n_{bi}^L) symbolizes the number of bonds per surface site that emanate from layer i in a direction perpendicular (parallel) to the surface. Order parameters of 1 and $-1/2$ correspond to situations of perfectly perpendicular and perfectly parallel bond orientation with respect to the surface. Bond order parameter profiles at the free surface are plotted in parts a and b of Figure 8 for n-decane and PDMS, respectively. In the highly attenuated surface region, consisting of the three top layers (compare Figure 7), the prevalent bond orientation is perpendicular to the surface; the few chains that participate in that region prefer directing their backbones along the z-axis to lying down parallel to the xy plane. In the fifth lattice layer, which is the first at which segment density is appreciable, the prevalent bond orientation becomes weakly parallel to the surface. It subsequently relaxes to its isotropic bulk characteristics within two or three layers. Profiles for the short-chain n-decane and for the long-chain PDMS are similar; the minimum in the fifth layer seems to be somewhat deeper in the short-chain case. An increase in system temperature is accompanied by a substantial de-

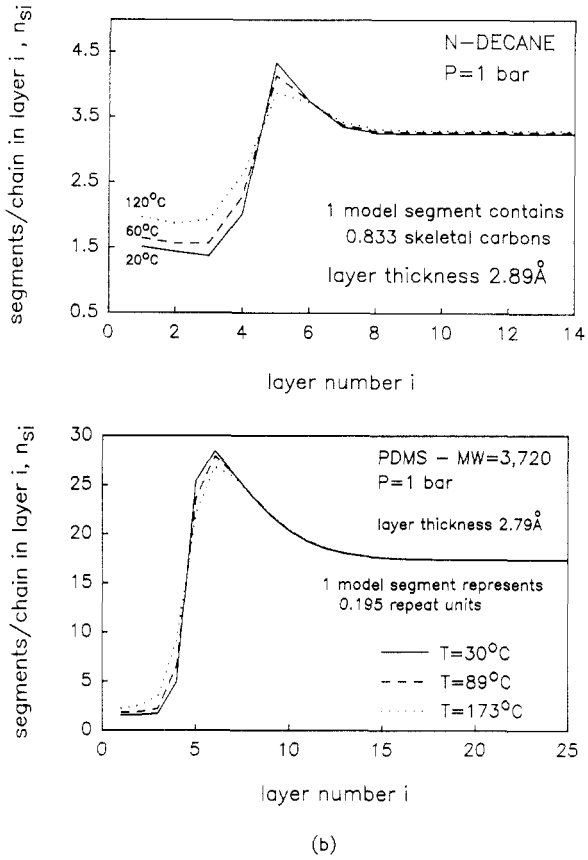

(b)

Figure 9. Chain shape profiles at the free surface of (a) *n*-decane and (b) a 50-unit poly(dimethylsiloxane). The quantity n_{si} stands for the average number of segments that a chain passing through layer *i* occupies in that layer.

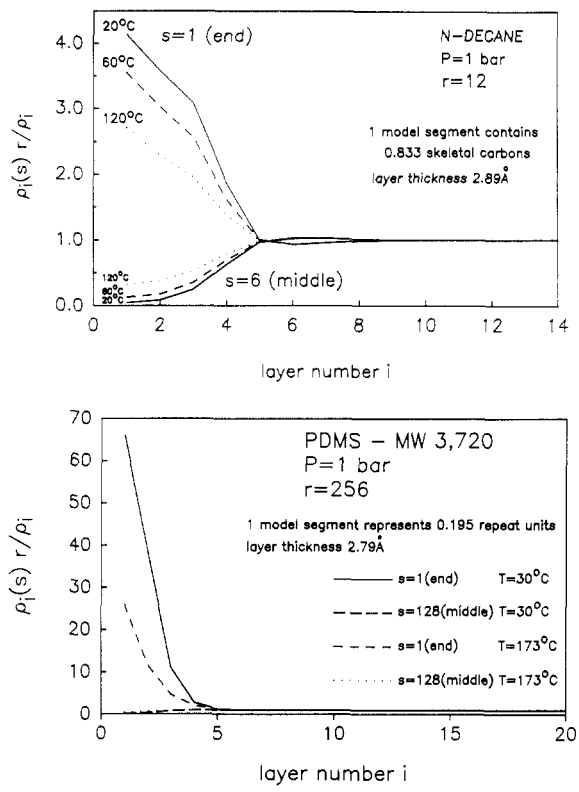

Figure 10. Spatial distribution of chain ends and middle segments in (a) *n*-decane and (b) in 50-unit poly(dimethylsiloxane). The dimensionless ratio $\rho_i(s)r/\rho_i$ is a measure of the local density of segments of order *s* relative to the overall local segment density (irrespective of segment order) in layer *i*. Values of $s = 1$ and $s = r/2$ correspond to chain ends and middle segments, respectively.

crease in bond orientation effects.

Chain Shape. The average width of chains participating in the various layers of the model lattice is plotted against layer number in parts a and b of Figure 9 for *n*-decane and PDMS, respectively. In the highly attenuated surface region, chains are very narrow (elongated in the *z* direction). They become pronouncedly flattened as one moves into the region of appreciable density. (A maximum in n_{si} is observed at $z = 15.9$ Å in the case of *n*-decane and at $z = 18.1$ Å in the case of PDMS.) Deeper in the fluid phase, the flattening disappears gradually, as conformations relax to their unperturbed bulk characteristics. The length, over which this flattening effect disappears, is clearly larger in the higher molecular weight system; it is commensurate with the end-to-end distance of an unperturbed coil. Temperature affects the distribution of chain shapes less than bond orientation. Conformations in the high molecular weight PDMS system, in particular, are rather insensitive to changes in temperature.

Distribution of Chain Ends and Middle Segments. As an additional measure of surface structure, we examine the spatial distribution of segments as a function of their topological position in the chain backbone. Numbering chain segments from $s = 1$ to $s = r$, we will use the symbol $\rho_i(s)$ to denote the local mass density (in g/cm^3) of segments of order *s* in layer *i*. With the simple homopolymer architectures examined, the following symmetry condition is satisfied:

$$\rho_i(s) = \rho_i(r-s+1) \quad (1 \le i \le m,\ 1 \le s \le r) \qquad (33)$$

The dimensionless ratio $\rho_i(s)r/\rho_i$ measures the extent to which the distribution of s-type segments departs from the overall mass distribution in the interfacial region. If the contents of layer *i* constitute a random mixture of segments of all orders, then the ratio $\rho_i(s)r/\rho_i$ will equal 1 for all *s*. Values of this ratio greater (less) than 1 indicate a concentration enhancement (depletion) of segments of order *s* in layer *i*.

The relative local density profiles $\rho_i(s)r/\rho_i$ in *n*-decane and PDMS are plotted in parts a and b of Figure 10 for segments of order $s = 1$ (chain ends) and segments of order $s = r/2$ (middle segments). A tendency for chain ends to preferentially concentrate in the highly attenuated surface region is evident in *n*-decane. Of the few segments that participate in the first layer of this model alkane surface at 20 °C, 69% are chain ends (i.e., model segments of orders $s = 1$ or $s = r$), even though end segments represent only 17% of the total chain mass. Conversely, middle segments avoid the highly attenuated surface region. Their density distribution displays a shallow peak in the sixth lattice layer. Deeper in the fluid, where overall density assumes its bulk value, segments of all orders are randomly distributed. The surface enhancement in chain ends actually becomes dramatic for the high molecular weight PDMS. Here, 51.5% of the total population of the first layer consists of chain ends, even though end segments represent only 0.8% of the total polymer mass. There are both energetic and entropic reasons for this enhancement in ends. Exposing a chain tail to the highly attenuated surface region is accompanied by a smaller loss of cohesive energy than exposing a middle segment, together with the loop of segments neighboring it on both sides. On the other hand, the conformational restriction associated with placing a chain tail adjacent to a plane surface is less severe than that resulting from pushing an entire train of internal segments against the surface. In both the *n*-decane and PDMS systems, the distributions of segments of given

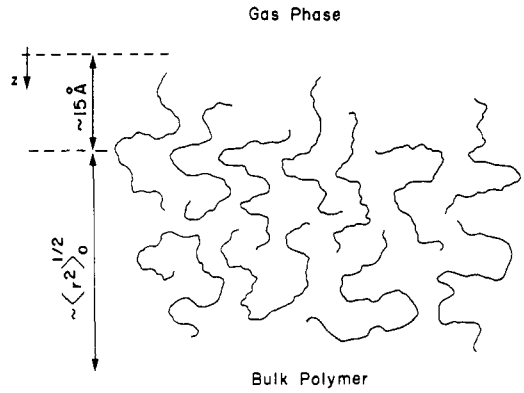

Figure 11. Pictorial representation of molecular structure at the free surface of a melt.

order become less inhomogeneous with increasing temperature.

The density, orientation, and conformation measures depicted in Figures 7–10 provide a self-consistent picture of free surface structure at the molecular level. A simplified representation of this structural picture is attempted in Figure 11. Sparse, hair-like, perpendicularly oriented tails reach out from the mobile mass of chains at the extremities of the polymer. Conformations are flattened, as surface chains try to take advantage of cohesive interactions in regions of appreciable density. The conformation assumes unperturbed characteristics as one moves into the bulk. This structural picture is quite consistent with molecular dynamics simulations of spontaneous cavitation in an *n*-octane-like fluid by Weber and Helfand.[29] Their work, which is based on an accurate representation of molecular geometry, and is free of the simplifying assumptions introduced in our lattice treatment, clearly shows a tendency for hydrocarbon chains to align perpendicular to a spherical vacuum/liquid interface, with their ends pointing toward the vacuum phase and their conformational distribution significantly enriched in trans states relative to the bulk.

4. Concluding Remarks

We have outlined a variable-density lattice model of polymer melt surfaces and polymer melt/solid interfaces. The model was designed to predict surface thermodynamic properties (surface tension, adhesion tension) and structural features at the molecular level, based on parameters determined independently from volumetric behavior in the bulk. Conformational energy (chain stiffness) effects can also be incorporated. We have applied the model to free surfaces of normal alkanes, linear polyethylene, and poly(dimethylsiloxane).

Surface tensions are underestimated by 28–40%, if the Sanchez–Lacombe equation of state parameters are used to represent these macromolecular systems. This is due primarily to the omission of the intersegmental interaction potential tails in the lattice model. The scaling of surface tension with molecular weight, however, is successfully predicted. Also, the temperature dependence of surface tension is captured very accurately by the model. This means that the relative significance of enthalpic vs entropic contributions to surface tension is correctly assessed.

The model provides a detailed and self-consistent picture of polymer structure at the molecular level. At a free polymer surface, the density falls from its bulk value to a value of practically zero along a sigmoidal profile that spans a thickness of ca. 15 Å. Sparse, perpendicularly oriented chain tails protrude into the highly attenuated surface region. Conformations become flattened as chains enter the region of appreciable density and gradually assume their unperturbed bulk characteristics over a distance commensurate with the mean squared end-to-end length.

We do not intend to convey the impression that the Sanchez–Lacombe equation of state and the interfacial model derived herein are perfect. First, the Sanchez–Lacombe model provides only an approximate, mean-field representation of the actual thermodynamics of a lattice fluid. Madden et al.[30] have recently addressed this question through Monte Carlo simulation; they find that the actual volumetric and phase behavior of a lattice fluid with given r, T^*, and P^* departs significantly from the prediction of the Sanchez–Lacombe model for the same parameter values and can only be reproduced by this model if r, T^*, and P^* are treated as adjustable parameters. Then, a discrete lattice is only an approximate representation of continuum systems. Problems associated with the omission of potential tails, and with the coordination number dependence of obtained results, have been pointed out in the discussion of our results. Nonlocal contributions to the free energy of the polymer film phase, which may be quite important,[31] are incorporated in our interfacial model only in a rudimentary way. Moreover, Dickman and Hall[32] have recently shown that the lattice-based Flory approximation for the insertion probability of chains, on which the Sanchez–Lacombe and Scheutjens–Fleer formulations are based, leads to an underestimation of pressure in hard-core chain fluids. Some limitations of the Sanchez–Lacombe equation in fitting data from polymer melts at high pressures have been pointed out by Dee and Walsh.[33] Despite these weaknesses, one must acknowledge that the Sanchez–Lacombe model performs very well in correlating experimental data at ordinary pressures.[2] Moreover, it is remarkable that the Sanchez–Lacombe picture of the polymer as a mixture of chains and voids can be coupled to a Scheutjens and Fleer type treatment of interfaces in a coherent statistical mechanical analysis that permits the detailed exploration of both thermodynamic and structural features, without invoking any phenomenological concepts foreign to the lattice representation. The formulation presented herein is thus useful in quickly exploring the salient features of polymer surfaces and polymer/solid interfaces and in deriving semiquantitative estimates of surface and interfacial tension. Detailed atomistic approaches to interfacial behavior that are free of the approximations involved in this treatment can be developed at a substantially higher computational cost.[34]

Results from applying our variable-density model to polymer melt/solid systems are reported in the following paper in this issue.

Acknowledgment. We are grateful for financial support by the IBM Corp., under a Shared University Research Program contract, Agreement No. SL 88037. Computational resources were made available through support provided by the Director, Office of Energy Research, Office of Basic Energy Sciences, Materials Science Division of the U.S. Department of Energy under Contract No. DE-AC03-76SF00098. The author deeply thanks the National Science Foundation for a Presidential Young Investigator Award, Grant No. DMR-8857659.

Symbols

a	surface area
a^*	area of a mole of surface sites: $a^* = N_L(l^*)^2$
G	Gibbs energy
h	thickness of interfacial polymer film
i	index for lattice layers
K	constant in correlation, eq 23
k	Boltzmann constant

l^* lattice edge length
L number of sites on each solid surface
m one-half of the number of layers in interfacial region
M chain molecular weight
n number of chains
n_{bi}^N number of bonds per surface site that connect layers i and $i+1$ and are therefore perpendicular to the interface
n_{bi}^L number of bonds per surface site that are parallel to the interface in layer i
n_c number of chains belonging to conformation c
n_{si} average number of segments per surface site that a chain passing through layer i occupies in that layer
N_L Avogadro number
P pressure
P^* Sanchez–Lacombe pressure parameter (characteristic pressure, indicative of the cohesive energy density of the polymer; equal to RT^*/v^*)
P_i "free segment probability" in layer i, defined in eq 7
$P(i,s)$ "end segment probability" for an s-segment-long subchain in layer i
r number of model segments in model chain
$r_{i,c}$ number of sites occupied by conformation c in layer i
r_u number of chemical units (mers) in actual chain
$\langle r^2 \rangle_0^{1/2}$ root mean squared unperturbed end-to-end distance
R ideal gas constant
s index for segments and bonds along a chain
S entropy
S_i bond order parameter in layer i
t thermometric temperature
T thermodynamic temperature
T_L temperature characteristic of short-range intramolecular energy associated with gauche placement of a bond, relative to trans
T_V temperature characteristic of short-range intramolecular energy associated with bond backstepping, relative to trans placement
T^* Sanchez–Lacombe temperature parameter (characteristic temperature of segment–segment interactions: $T^* = -(zw_{AA}/2k)$)
T_s^* characteristic temperature of segment–surface interactions: $T_s^* = -(w_{AS}/k)$
U internal energy
v^* volume of 1 mol of chain segments: $v^* = N_L(l^*)^3$
V volume
w_{AA} energy of attractive interactions between segments occupying nearest-neighbor sites in the lattice
w_{AS} energy of attractive interactions between adsorbed polymer segments and surface sites
x coordinate axis parallel to surface
y coordinate axis parallel to surface
$Y(i,s)$ intramolecular energy factor in segment balance equations, eq 8
z lattice coordination number, $z = 6$; coordinate axis perpendicular to interface

Greek Symbols

γ surface tension of pure polymer; interfacial tension in polymer–solid system
γ_s surface tension of clean solid
δ_{ij} Kronecker δ
δ_s distance over which variations in solid structure at the interfacial region are observed
ϵ intramolecular (conformational) potential energy for a pair of adjacent bonds along a chain, relative to trans placement
ϵ_c total intramolecular (conformational) energy of a chain in conformation c
λ_0 fraction of nearest-neighbor sites to a given site lying in same layer as the considered site
λ_1 fraction of nearest-neighbor sites to a given site lying in layer above (i.e., nearer the surface) the layer of the considered site; fraction of nearest-neighbor sites to a given site lying in layer below the layer of the considered site
ξ Lagrange multiplier associated with chain balance constraint
ρ polymer mass density
$\rho_i(s)$ contribution to density of polymer in layer i due to segments of order s
τ Boltzmann factor, corresponding to the energy of a conformational state
φ polymer volume fraction
χ segment–segment interaction parameter, defined in eq 5
χ_s segment–surface interaction parameter, defined in eq 5
Υ availability (thermodynamic property, defined in eq 3)
ω_c factor proportional to the number of arrangements of conformation c on the lattice, defined in ref 7

Subscripts

A polymer segment
b unconstrained bulk polymer phase
f interfacial polymer (film) phase
i lattice layer index
L gauche placement of a bond relative to previous bond
N normal component of pressure (perpendicular to surface)
s nonpolymer (solid or gaseous) phase
s index for bonds and segments
sb bulk solid, in the absence of surfaces
S surface site
T transverse component of pressure (parallel to surface)
V backstepping placement of a bond relative to previous bond
α index for phases
∞ infinite molecular weight

Special Symbols

$\bar{}$ mean value over entire film phase thermodynamic quantity
$\hat{}$ total (as opposed to molar or specific) extensive thermodynamic quantity
$\langle\ \rangle$ ensemble average

Registry No. C_6, 110-54-3; C_7, 142-82-5; C_8, 111-65-9; C_9, 111-84-2; C_{10}, 124-18-5; C_{12}, 112-40-3; C_{14}, 629-59-4; C_{17}, 629-78-7; polyethylene, 9002-88-4.

References and Notes

(1) Scheutjens, J. M. H. M.; Fleer, G. J. *J. Phys. Chem.* **1979**, *83*, 1619; **1980**, *84*, 178; *Macromolecules* **1985**, *18*, 1882.
(2) Sanchez, I. C.; Lacombe, R. H. *J. Chem. Phys.* **1976**, *80*, 2352; *Polymer Lett.* **1977**, *15*, 71; *Macromolecules* **1978**, *11*, 1145.
(3) Ramamurthy, A. V. *Adv. Polym. Technol.* **1986**, *6*, 489; *J. Rheol.* **1986**, *30*, 337.
(4) Helfand, E. *Macromolecules* **1976**, *9*, 307. Weber, T. A.; Helfand, E. *Macromolecules* **1976**, *9*, 311.
(5) Madden, W. G. *J. Chem. Phys.* **1987**, *87*, 1405.
(6) Poser, C. I.; Sanchez, I. C. *J. Colloid Interface Sci.* **1979**, *69*, 539.
(7) Theodorou, D. N. *Macromolecules* **1988**, *21*, 1400.
(8) Gubbins, K. E. In *Fluid Interfacial Phenomena*; Croxton, C. A., Ed.; Wiley: New York, 1986; p 469.
(9) Navascués, G.; Berry, M. V. *Molec. Phys.* **1977**, *34*, 649.
(10) Magda, J. J.; Tirrell, M. V.; Davis, H. T. *J. Chem. Phys.* **1985**, *83*, 1888.
(11) Modell, M.; Reid, R. C. *Thermodynamics and Its Applications*, 2nd ed.; Prentice Hall: Englewood Cliffs, 1983; p 410.
(12) The thermodynamic notation adopted here deserves some comment. A circumflex will denote total (extensive) properties. Symbols without a circumflex will denote molar or intensive properties. Thus, $\hat{V}$ is a total volume, in m^3, whereas V is a molar volume, in m^3/mol.
(13) Theodorou, D. N. *Molecular Thermodynamics of Polymer Melts at Interfaces*; Research Report, Center for Advanced Materials, Lawrence Berkeley Laboratory: Berkeley, 1988 (LBL-26018).
(14) DiMarzio, E. A.; Rubin, R. J. *J. Chem. Phys.* **1971**, *55*, 4318.

(15) Leermakers, F. A. M.; Scheutjens, J. M. H. M.; Gaylord, R. J. *Polymer* **1984**, *25*, 1577.
(16) Kurata, M.; Isida, S.-I. *J. Chem. Phys.* **1954**, *23*, 1126.
(17) van Voorhis, J. J.; Craig, R. G.; Bartell, F. E. *J. Phys. Chem.* **1957**, 1513.
(18) Ash, S. G.; Everett, D. H.; Radke, C. *J. Chem. Soc., Faraday Trans. 2* **1973**, *69*, 1256.
(19) Helfand, E.; Sapse, A. M. *J. Polym. Sci., Polym. Symp.* **1976**, *54*, 289.
(20) Ploehn, H. J.; Russel, W. B.; Hall, C. K. *Macromolecules* **1988**, *21*, 1075.
(21) Rabin, Y. *J. Polym. Sci., Polym. Lett. Ed.* **1984**, *22*, 335.
(22) Bongiorno, V.; Scriven, L. E.; Davis, H. T. *J. Colloid Interface Sci.* **1976**, *57*, 462.
(23) Jasper, J. J. *J. Phys. Chem. Ref. Data* **1972**, *1*, 841.
(24) Legrand, D. G.; Gaines, G. L. *J. Colloid Interface Sci.* **1969**, *31*, 162.
(25) Roe, R.-J. *J. Phys. Chem.* **1968**, *72*, 2013.
(26) Van Krevelen, D. W. *Properties of Polymers*; Elsevier: Amsterdam, 1976.
(27) Hillstrom, K. *Nonlinear Optimization Routines in AMDLIB*; Technical Memorandum No. 297, Argonne National Laboratory, Applied Mathematics Division, 1976; Subroutine SBROWN in AMDLIB, 1976, Argonne, IL.
(28) Flory, P. J. *Statistical Mechanics of Chain Molecules*; Interscience: New York, 1969.
(29) Weber, T. A.; Helfand, E. *J. Chem. Phys.* **1980**, *72*, 4014.
(30) Madden, W. G.; Pesci, A. I.; Freed, K. F., submitted to *J. Chem. Phys.*
(31) Professor Matthew Tirrell, personal communication.
(32) Dickman, R. D.; Hall, C. K. *J. Chem. Phys.* **1986**, *85*, 4108.
(33) Dee, G. T.; Walsh, D. T. *Macromolecules* **1988**, *21*, 811, 815.
(34) Mansfield, K. F.; Theodorou, D. N. *Polym. Prepr. (Am. Chem. Soc., Div. Polym. Chem.)* **1988**, *29*(2), 409.

Variable-Density Model of Polymer Melt/Solid Interfaces: Structure, Adhesion Tension, and Surface Forces

Doros N. Theodorou

Department of Chemical Engineering, University of California, Berkeley, and Center for Advanced Materials, Lawrence Berkeley Laboratory, Berkeley, California 94720.
Received December 27, 1988; Revised Manuscript Received April 24, 1989

ABSTRACT: A recently developed variable-density lattice model is used to predict the macroscopic wetting and spreading behavior of a polymeric liquid on smooth solid surfaces. The force field exerted by the solid affects structural features in the interfacial region. Near strongly adsorbing, "high-energy" solids, polymer density is enhanced relative to the bulk. Conformations are pronouncedly flattened; they relax monotonically to their unperturbed characteristics over a thickness commensurate with the root mean squared end-to-end distance. Near weakly adsorbing solids, polymer density is depleted due to entropic restrictions, and structure is reminiscent of a free polymer surface. A thermodynamic formulation is developed for predicting the forces exerted between molecularly smooth solid surfaces immersed in polymeric liquids, at separations commensurate with chain dimensions. The system considered is a monodisperse 50-unit poly(dimethylsiloxane) between smooth flat plates or crossed cylinder surfaces of various adsorbing strengths. In the case of high-energy solid surfaces, which are most representative of the mica actually used in surface force experiments, the model predicts repulsive forces of negligible magnitude (on the order of 1 μN/m) due to the polymer. The model indicates that the long-range repulsive forces observed recently with higher molecular weight polymer melts are nonequilibrium (hydrodynamic) in nature.

1. Introduction

Understanding the structure and thermodynamics of macromolecular liquids in the vicinity of solid surfaces is important in technical areas such as adhesion, lubrication, and polymer melt processing. A quantitative theory, relating the chemical constitution of polymer chains and the composition and topography of solid surfaces to macroscopic interfacial properties, would be valuable as a tool for the efficient design of multiphase materials containing polymers. With the trend toward miniaturization that prevails in present-day high-technology areas, the need to understand interfacial properties at the molecular level becomes imperative. Polymer phases are becoming so thin that their behavior can no longer be satisfactorily described by continuum approaches.

In a companion paper,[1] we have outlined a variable-density, mean field lattice theory of polymer melt surfaces and polymer melt/solid interfaces. We have also presented some applications to free polymer melt surfaces. Our purpose in this paper is to explore systems involving polymer melt/solid interfaces. Such interfaces have scarcely been examined theoretically, although, from the point of view of applications, they are more interesting than free polymer surfaces. The material presented herein falls under three general headings. Section 2 addresses the problem of predicting molecular organization and adhesion tension at interfaces between a bulk polymer phase and a smooth solid. Section 3 is concerned with very thin polymer films, formed between smooth solid surfaces immersed in a macromolecular liquid. Forces between such surfaces at separations commensurate with chain dimensions have recently been measured; we apply our lattice approach to predict these forces at thermodynamic equilibrium. Results obtained in the bulk melt/solid interface case and in the confined thin-film case are discussed in section 4.

2. Modeling the Polymer Melt/Solid Interface

Adhesion Tension. As described in the preceding paper in this issue, our interfacial model combines ideas from the equation of state work of Sanchez and Lacombe[2] and from the Scheutjens and Fleer model of polymer adsorption from solution on solid surfaces.[3] The chemical constitution of the polymer is summarized in three molecular parameters: the chain length r, the characteristic temperature of cohesive segment–segment interactions T^*, and the characteristic pressure P^*, from which segmental volume can be extracted. Conformational energy (chain stiffness) effects will not be considered in any of the calculations reported in this paper. Attractive segment/solid interactions, characterized in our lattice model by the parameter T_s^*, play a decisive role in shaping the interfacial picture. All computations in this section were performed with a film thickness h large enough that the

0024-9297/89/2222-4589$01.50/0